Regular Article

PHYSICAL CHEMISTRY RESEARCH
Published by the
Iranian Chemical Society
www.physchemres.org
info@physchemres.org

***Phys. Chem. Res.**, Vol. 4, No. 2, 271-283, June 2016*
DOI: 10.22036/pcr.2016.13969

Influence of a Novel Magnetic Recoverable Support on Kinetic, Stability and Activity of Beta-amylase Enzyme

N. Rasouli*, N. Sohrabi* and M. Zamani
Department of Chemistry, Payame Noor University, P.O. Box: 19395-3697, Tehran, Iran
(Received 10 January 2016, Accepted 22 March 2016)

In this paper, covalent immobilization of beta amylase enzyme on the surface of modified magnetic nano particles ($ZnFe_2O_4$@SiO_2-NH_2) is reported. For doing so, at first, the magnetic nanoparticles of $ZnFe_2O_4$ were synthesized by chemical co-precipitation method and then tetraethyl orthosilicate (TEOS) and 3-aminopropyltriethoxy silane (APTES) were used for modification of $ZnFe_2O_4$ nanoparticles with silica and amine groups ($ZnFe_2O_4$@SiO_2-NH_2). Then, the aminated surface of $ZnFe_2O_4$ nanoparticles was exposed to beta amylase immobilization using trichlorotriazine (TCT) as covalent agent. The immobilized beta-amylase enzyme was characterized by techniques such as Fourier transform infrared (FT-IR), scanning electron microscopy (SEM), powder X-ray diffraction (XRD) and energy dispersive X-ray analysis (EDAX). The kinetics studies corroborate the Michaelis-Menten model and show much progress in the efficiency of immobilized enzyme compared to the free enzyme. Also, the thermal stability of the beta-amylase enzyme is increased after immobilization. By applying a magnetic active support, simple and facile separation of beta-amylase from the reaction mixture and higher catalytic activity is possible. The highest activity for immobilized beta-amylase enzyme is observed at pH and temperature of 7.0 and 40 °C, respectively.

Keywords: Immobilization, Beta-amylase, Magnetic support, Kinetic

INTRODUCTION

The use of enzymes in industrial scale due to their high costs, low stability and reusability is limited. So, immobilization of enzymes on different supports increases the stability and reusability of enzyme. In recent years, research on magnetic nano particles has been of high importance because of their specific structure, low toxicity, easy synthesis and high magnetic response to an external magnetic field [1-6]. Also, magnetic nano particles show high potential in various fields including separation of proteins, cell labeling, drug delivery and catalysis [7-10]. Recent studies show that magnetic nano particles possess a great potential for the immobilization of enzyme that include enzyme reusability using an external magnetic field [11-15]. Also, when the particle size is reduced, high surface-to-volume ratio is obtained, which led to high-capacity for enzyme immobilization [15,16]. In addition, compared with porous compounds when using magnetic nano particles for enzyme immobilization, there is not limitation for diffusion of substrates and products [11-13]. Also, the covalent bond between the enzyme and support has benefits that include reducing of conformational change involved in enzyme inactivation and increasing enzyme stability [16,17]. Beta-amylase enzyme attacks the alpha-1,4-glucan bond localized on the non-reducing ends of starch and transforms it to maltose units. Maltose, a disaccharide formed from two units of glucose is widely used in food and pharmaceutical industries [18-22]. For example, the sweetness properties of the traditional sweet potato is related to maltose produced *via* beta-amylase enzyme [23,24]. The main objective of this work is to develop a magnetically responsive support which enables

*Corresponding author. E-mail: n.rasouli@pnu.ac.ir;

the better reuse of the enzyme to the magnetic substrate as well as the better reuse of the enzyme using a magnetic field. The results show that surface-modified $ZnFe_2O_4$ magnetic nano particles are promising support for beta-amylase enzyme immobilization.

EXPERIMENTAL

Materials and Methods

The materials used, including beta-amylase (EC 3.2.1.1), tetraethyl orthosilicate (TEOS), 3-aminopropyltriethoxy-silane (APTES), trichlorotriazine (TCT), 3,5-dinitrosalicylic acid (DNS), Maltose, Starch, Sodium Potassium Tartrate ($KNaC_4H_4O_6.4H_2O$), sodium dihydrogen phosphate and disodium hydrogen phosphate, ferric nitrate nonahydrate ($Fe(NO_3)_3{\cdot}9H_2O$), zinc nitrate hexahydrate ($Zn(NO_3)_2.6H_2O$) and ammonium hydroxide (25%), were purchased from Sigma-Aldrich.

Instruments Used

The morphology of the samples were analyzed by field emission scanning electron microscope (FE-SEM, Hitachi S-4160). The FT-IR absorption spectra were recorded on KBr pellets of samples in the range of 4000-400 cm^{-1} using a JASCO FT-IR-4200 spectrophotometer. The X-ray diffraction measurement was recorded on an X-ray diffractmeter Bruker, D8ADVANCE using Cu Kα radition (λ = 0.1540 nm) and the EDX spectra were recorded by Energy-dispersive X-ray spectroscopy (EDX) (Philips XL 30).

Synthetic Procedure of $ZnFe_2O_4$ Nanoparticles

Although various methods have been reported for the synthesis of magnetic nano particles in the literature [25-27], the chemical co-precipitation method as a simple and fast method was used in this study. According to this method, 1.25 g of $Zn(NO_3)_2.6H_2O$ and 3.4 g of $Fe(NO_3)_3{\cdot}9H_2O$ with molar ratio 1:2 were dissolved in 100 ml deionized water and heated to 60 °C, then 6 ml of ammonium hydroxide (25%) was added to the solution and the mixture stirred for 30 min. The formed brown precipitate was washed with deionized water and ethanol [28].

Preparation of Silica Coated $ZnFe_2O_4$ Nanoparticles

The classical Stöber method was used for modifying of $ZnFe_2O_4$ nano particles with a silica shell ($ZnFe_2O_4@SiO_2$) [29]. The amount of 0.145 g of $ZnFe_2O_4$ nano particles with 40 ml of ethanol was mixed and ultrasonicated for 10 min. Then, 6 ml of water and 3 ml of ammonium hydroxide solution were added and followed by addition of 4 ml tetraethyl orthosilicate (TEOS) was stirred at room temperature for 5 h. The obtained silica-coated $ZnFe_2O_4$ nano particles were washed several times with ethanol and water and dried under vacuum at room temperature.

Surface Modification of Silica-coated $ZnFe_2O_4$ Nanoparticles

The surface modification of silica-coated $ZnFe_2O_4$ nano particles was carried out by Wang and Liu *et al.* method [30]. The obtained silica-coated $ZnFe_2O_4$ nano particles (5 mg) were treated with 3-aminopropyltriethoxysilane (APTES) (300 µl) in ethanol (500 µl) and the mixture was stirred at room temperature for 2 h, then was heated at 50 °C for 1.5 h. The amine-modified nanoparticles were separated from the cooled mixture by an external magnet and washed with ethanol and THF. Then, the obtained product were reacted with trichlorotriazine (TCT) (40 mg) in THF (1000 µl) at room temperature for 3 h. Finally, the obtained product ($ZnFe_2O_4@SiO_2$-NH_2-TCT) were washed with THF, ethanol and de-ionized water and dried under vacuum at room temperature.

Beta-amylase Immobilization

10 mg of the modified $ZnFe_2O_4$ nano particles synthesized in the previous step was dispersed in 800 µl phosphate buffer (20 mM, pH = 7.0). Then, various amounts of the beta-amylase enzyme solution (50-300 µg) were added to the solution and shaken at room temperature for 6 h. The immobilized beta-amylase enzyme was removed by a magnetic field and then washed with phosphate buffer to remove the free enzyme molecules from the surface. The wash solution was collected to determine the amount of immobilized beta-amylase enzyme on the surface of the modified $ZnFe_2O_4$ magnetic nano particles. Finally, the immobilized beta amylase enzyme was dried in vacuum oven at 40 °C and then stored in a vacuum desiccator [31].

The Immobilization Efficiency

The amount of the immobilized beta-amylase enzyme on the surface of the modified $ZnFe_2O_4$ magnetic nano particles was determined using the Bradford method [32]. After the immobilization process, the soluble portion was collected to calculate the amount of immobilized enzyme. For the same purpose, an enzyme calibration curve was plotted with different concentrations of enzyme using a starch solution with concentration of 1 mg ml^{-1}. The immobilization efficiency was evaluated by the variations in the concentrations of the soluble portion before and after the immobilization process. The amount of weakly adhered enzyme was taken into account while calculating the immobilization efficiency. The immobilization efficiency was found to be 60%.

Beta Amylase Activity

The free and immobilized enzyme activities were calculated according to the Bernfeld method [33]. The efficiency of starch hydrolysis by the free and immobilized enzymes was carried out by the reaction of 0.5 ml starch solution (concentration being 1%) with 20 mM phosphate buffer (pH = 7.0). Then, to this solution, 0.5 ml of the beta-amylase enzyme solution was added and incubated at 40 °C for 5 min. The reaction of starch hydrolysis was stopped by adding DNS reagent. Then, the solution was heated by boiling water bath for about 5 min. The dark red colored solution obtained was cooled to room temperature and was diluted suitably before recording of visible spectrum. Finally, the amount of reducing sugar produced was determined spectrophotometrically by recording of the absorbance at the wavelength of 540 nm. Beta-amylase activity is expressed as micromoles of maltose produced in unit time under the optimal conditions. The quantity of maltose liberated during the reaction was determined from maltose standard curve using DNS method. Under the same conditions, the examination for the immobilized enzyme was performed. The immobilized enzyme activity is determined by applying a magnetic field. The suitable reaction parameters such as pH and temperature for both the free and immobilized enzymes were deduced using the same procedure.

Thermal and pH Stability

The thermal stability of the free and immobilized beta-amylase enzyme was determined by measuring the residual enzyme activity after 30 min incubation in phosphate buffer (20 mM, pH = 7.0) and at temperature range of 30-70 °C. The pH stability was determined by measuring the residual enzyme activity after 30 min incubation at specified pH. This parameter was investigated in the pH range between 4-8.

Kinetic Parameters

The kinetic parameters of the free and immobilized beta-amylase enzyme were determined by measuring the initial rates of enzymes at different concentration of substrate (starch concentration (10-60 mM)). The K_m and V_{max} values were calculated using Lineweaver-Burk plot.

Storage Stability

The storage time of stability for the free and immobilized beta-amylase enzyme was determined at different times (1-12 days). The residual enzyme activity was calculated as percentage of the initial enzyme activity.

RESULTS AND DISCUSSION

Characterization

Figure 1 shows the FT-IR spectra of the surface modified $ZnFe_2O_4$ nano particles ($ZnFe_2O_4$@SiO_2-NH_2-TCT) with and without immobilized beta-amylase enzyme. In the FT-IR spectrum of $ZnFe_2O_4$, two characteristic peaks observed at around 410 and 549 cm^{-1} correspond to intrinsic stretching vibrations of the metal at the octahedral and tetrahedral sites, respectively [34,35]. In Fig. 1, the broad band around 3400.11 cm^{-1} and 1621.01 cm^{-1} can be assigned to O-H stretching vibrations of water. The peaks at 1092.48 cm^{-1} and 2915.84 cm^{-1} correspond to symmetric stretching of Si-O-Si and C-H, respectively. The peak at 1613.55 cm^{-1} correspond to -C=N- bond indicating the presence of TCT agent. After immobilization of beta-amylase enzyme on the surface of modified $ZnFe_2O_4$ nanoparticles, the peaks at 1695.2 cm^{-1} and 1711.51 cm^{-1} region correspond to formation of peptide bond. The results show that beta-amylase enzyme present in the samples and confirmed the binding of beta-amylase enzyme onto the surface of modified $ZnFe_2O_4$ nano particles. The powder X-ray diffraction (XRD) patterns were used to identify the

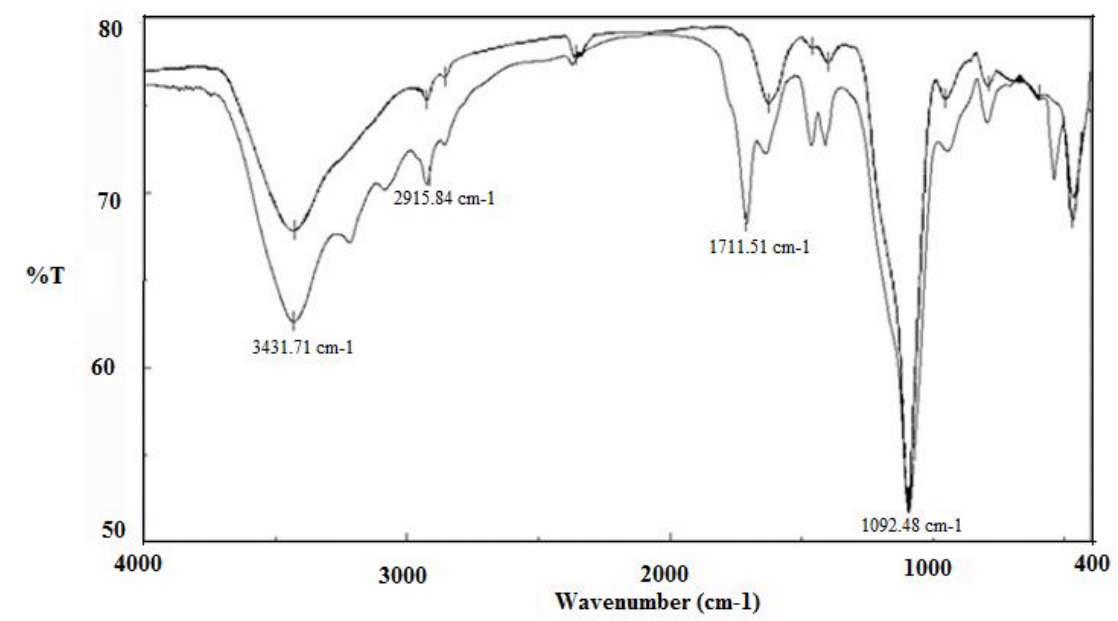

Fig. 1. FT-IR spectra of $ZnFe_2O_4$@SiO_2-NH_2-TCT (a) without and (b) with immobilization of beta-amylase enzyme.

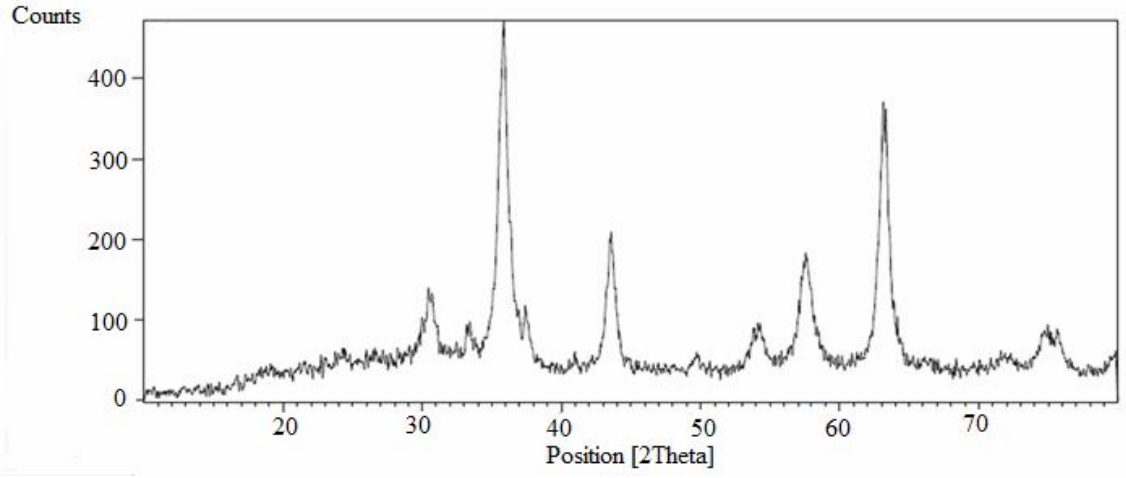

Fig. 2. XRD pattern of the $ZnFe_2O_4$ nanoparticles.

crystalline structure of $ZnFe_2O_4$ magnetic nanoparticles. The pure $ZnFe_2O_4$ is in the spinel phase (JCPDS No. 77-0011) and the distinctive peaks at 29.92°, 35.27°, 42.85°, 53.11°, 56.63° and 62.21° matched well with the reported data and can be indexed to pure phase of $ZnFe_2O_4$ structure (Fig. 2). The average crystallite size of the $ZnFe_2O_4$ nanoparticles calculated from Scherer's equation was 37 nm. The EDX spectrum of silica-coated $ZnFe_2O_4$ nano particles is shown in Fig. 3. The atomic weight ratio of O:Si:Fe was 36.31:29.47:34.22, which indicates the $ZnFe_2O_4$ nanoparticles are successfully modified by silica shell. The surface morphology of $ZnFe_2O_4$@SiO_2 and $ZnFe_2O_4$@SiO_2-NH_2-TCT is shown in the SEM images (Figs. 4a and 4b). In the SEM image of $ZnFe_2O_4$@SiO_2, the spherical

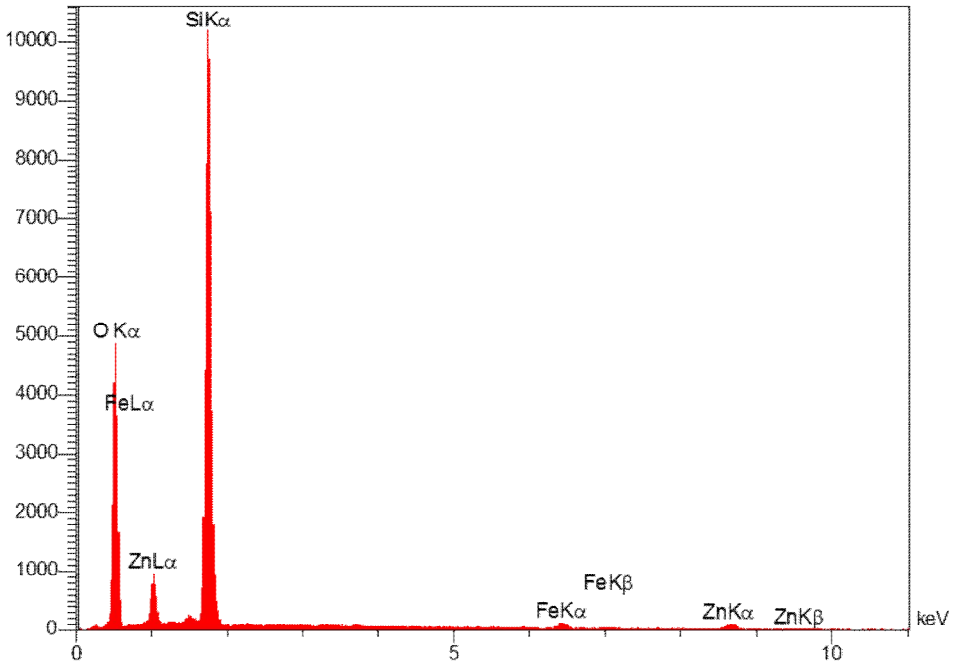

Fig. 3. EDX spectrum of silica-coated $ZnFe_2O_4$ nanoparticles.

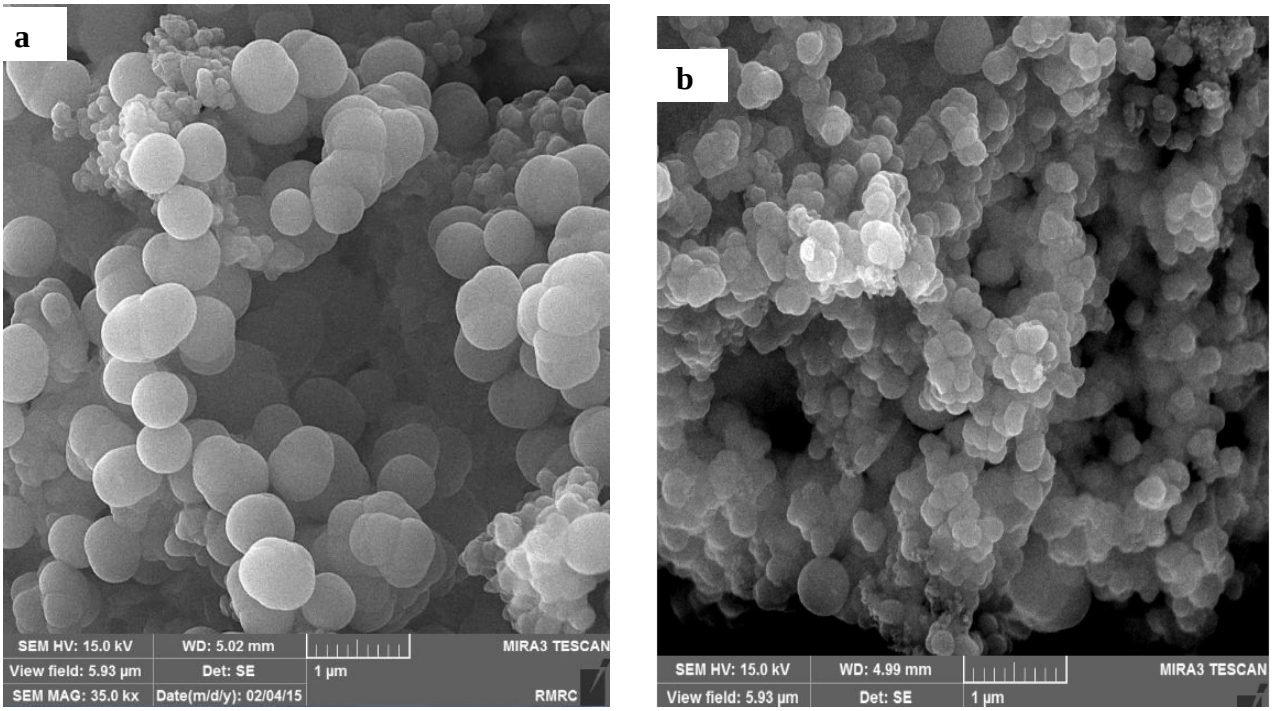

Fig. 4. SEM images of (a) $ZnFe_2O_4@SiO_2$ (b) $ZnFe_2O_4@SiO_2$-NH_2-TCT.

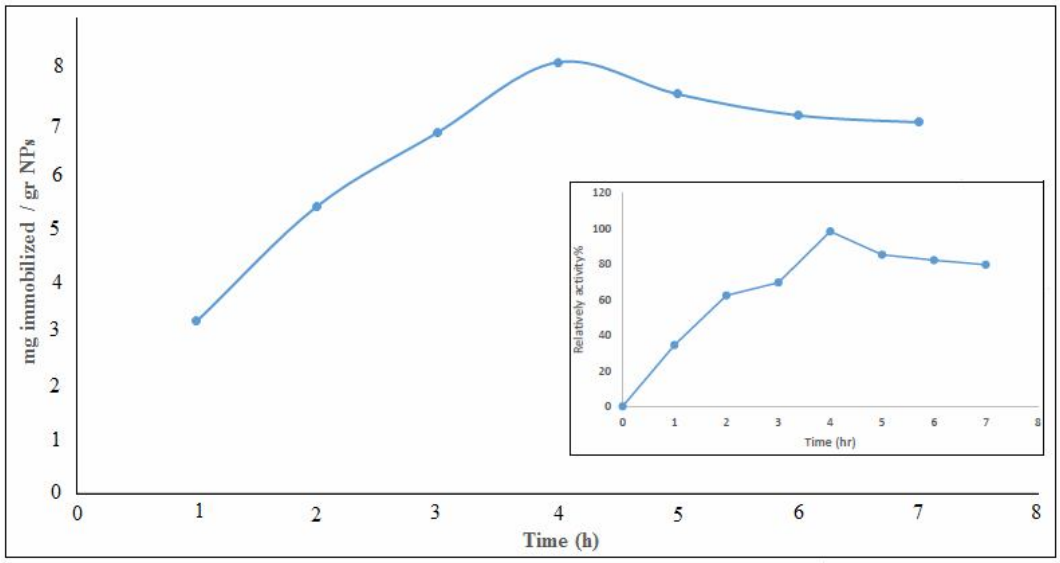

Fig. 5. The amount of immobilized beta-amylase enzyme and relative activity of immobilized beta-amylase enzyme versus the reaction time. Immobilization conditions: the initial amount of beta-amylase: 50 µg, 10 mg of $ZnFe_2O_4$ nanoparticles in 20 mM phosphate buffer (pH = 7.0, t = 25 °C).

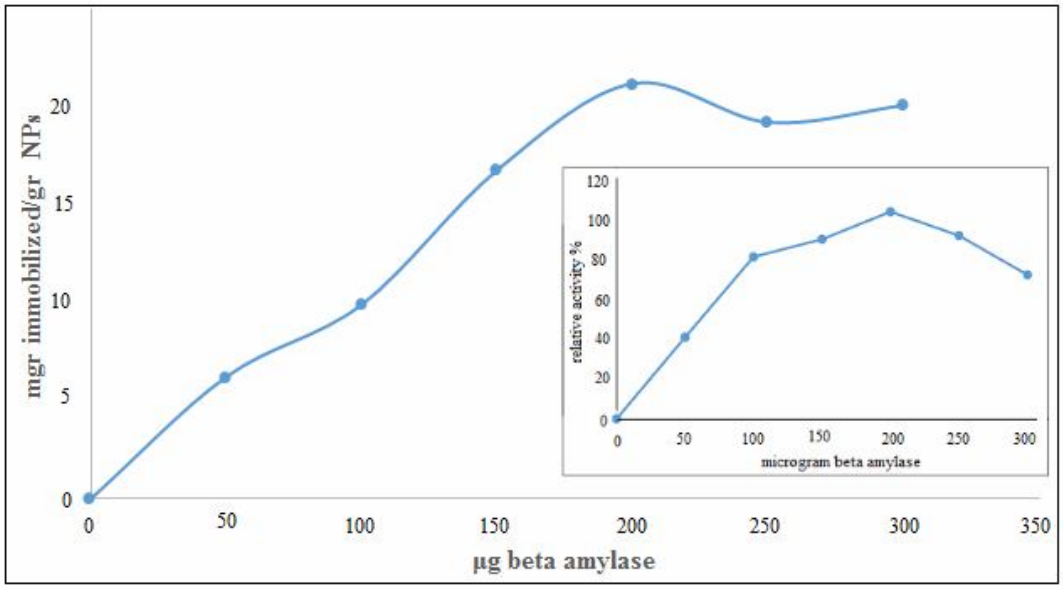

Fig. 6. Effect of the initial amount of beta-amylase on the amount of immobilized beta-amylase and the effect of different amounts of the beta-amylase added on relative activity of the immobilized beta-amylase. Immobilization conditions: t = 4 h, 10 mg of $ZnFe_2O_4$ nanoparticles in 20 mM phosphate buffer (pH = 7.0, t = 25 °C).

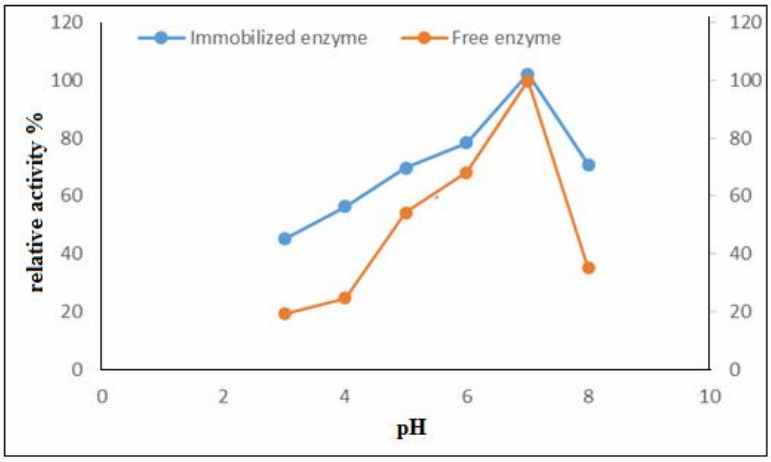

Fig. 7. Effect of pH on the catalytic activity (the amount of beta-amylase: 150 µg , 10 mg of $ZnFe_2O_4$ nanoparticles in 20 mM phosphate buffer (pH = 4.0-8.0, t = 25 °C).

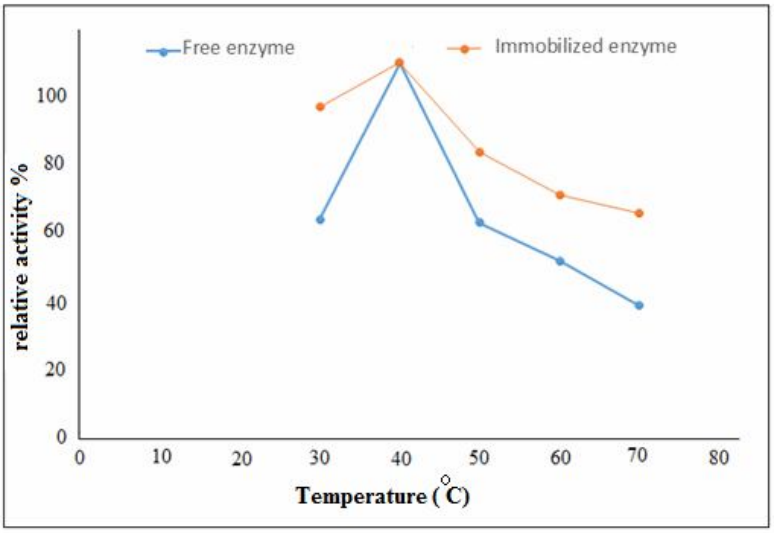

Fig. 8. Effect of temperature on the catalytic activity (the amount of beta -amylase: 150 µg, 10 mg of $ZnFe_2O_4$ nanoparticles in 20 mM phosphate buffer (pH = 7.0, t = 30-70 °C).

agglomerated silica particles are seen but the surface morphology is changed after modification with 3-aminopropyltriethoxy silane and trichlorotriazine agents.

BETA-AMYLASE IMMOBILIZATION PARAMETERS

Time of Immobilization

The amount of immobilized beta-amylase enzyme and its relative activity versus reaction time are shown in Fig. 5. The results showed that by increasing the reaction time from 1-4 h, the amount of immobilized beta-amylase enzyme increased and remained constant after about 5 h. Also, the results showed that the relative activity of beta-amylase enzyme was increased with reaction time up to 4 h and then decreased. The obtained results can be related to the saturation of trichlorotriazine (TCT) groups on the surface of $ZnFe_2O_4$ magnetic nano particles by beta-amylase

enzyme molecules after 4 h and reduction of enzyme activity after this time due to denaturation.

Concentration of Beta-amylase

The effect of various amounts of the beta-amylase enzyme (50-300 μg) located on modified $ZnFe_2O_4$ magnetic nanoparticles and following that the relative activity of the immobilized beta-amylase are shown in Fig. 6. The amount of the beta-amylase enzyme loading increased greatly with the initial concentration of beta-amylase enzyme and the relative activity reached a maximum value at 150 μg of beta-amylase enzyme. It is considered that the higher beta-amylase loading form intermolecular steric hindrance, which restrains the diffusion of the substrate and product. Therefore, the relative activity decreased slowly above 150 μg of beta-amylase,because the binding sites on the surface of the modified magnetic nano particles are limited and the enzyme molecules need enough space for catalyzing the reaction of the substrate.

Effect of pH

The role of pH on the catalytic activity of the free and immobilized beta-amylase enzyme was investigated in the range of pH = 4.0-8.0. Figure 7 shows the relative enzyme activity versus pH. As shown in Fig. 7, the pH of maximum activity for both the free and immobilized enzyme was found to be 6.5. The results show that the immobilized beta-amylase enzyme is more stable than the free enzyme. Also, it can be deduced that the better activity for beta-amylase enzyme is not observed at lower and higher values of pH, which could be due to the changes in the enzyme structure in presence of excessive ions.

Effect of Temperature

The effect of temperature on the activity of the free and immobilized enzyme was studied under 150 μg of beta-amylase enzyme, 10 mg $ZnFe_2O_4$ magnetic nano particles in 20 mM phosphate buffer (pH = 7.0) and at various temperatures (t = 30-70 °C) (Fig. 8). The results showed that the relative activity loss was approximately 51.45% and 75.65% for the immobilized enzyme and free enzyme, respectively. The activity of the immobilized enzyme was higher than that of the free enzyme at elevated temperatures, suggesting that the immobilization improves the thermal stability of the enzyme significantly.

Storage Stability

Figure 9 shows the storage stability of the immobilized enzyme stored in 20 mM phosphate buffer (pH = 7.0) at 4 °C and its activity was tested for 12 days. The immobilized enzyme retained 79.99% of its activity after 12 days, but the free enzyme retained 40.61% of its activity after 12 days. The obtained results showed that the immobilized enzyme was more stable than the free enzyme.

Kinetic Parameters for Immobilized and Free Enzyme

The kinetic studies for the free and immobilized enzymes was carried out by hydrolysis of soluble starch solution in various concentrations. The Michaelis-Menten plots (rate of the reaction *vs.* substrate concentration) are shown in Fig. 10. Also, the Lineweaver-Burk plot was drawn to determine the V_{max} and K_m values for both the free and immobilized enzymes. The results showed that the free and immobilized enzymes follow the Michaelis-Menten kinetics model, which is reflected in the adjacent R^2 values (close to unity), presented in the inset of Figs. 11a and 11b. From the kinetic experiments, the V_{max} values for the free and immobilized enzymes are found to be 4.81 and 12.63 μmol ml^{-1} min^{-1}, respectively. The Michaelis-Menten constants (K_m) for the free and immobilized enzymes are 7.49 and 5.64 mM, respectively.

Recycling Efficiency of the Immobilized Enzyme

Due to the advantages of immobilization of enzymes on different supports, the immobilized beta-amylase enzyme was examined for the repeated catalytic use after its recovery magnetically. Figure 12 showed the relative activity of the enzyme in terms of the number of cycles. The activity of the immobilized beta-amylase enzyme is found to slowly reduce after the first cycle. The results showed that the immobilized beta-amylase enzyme remained 83% of its initial activity after six cycles. The decrease in the bio catalytic activity might be due to slow denaturation of the enzyme during repeating handling.

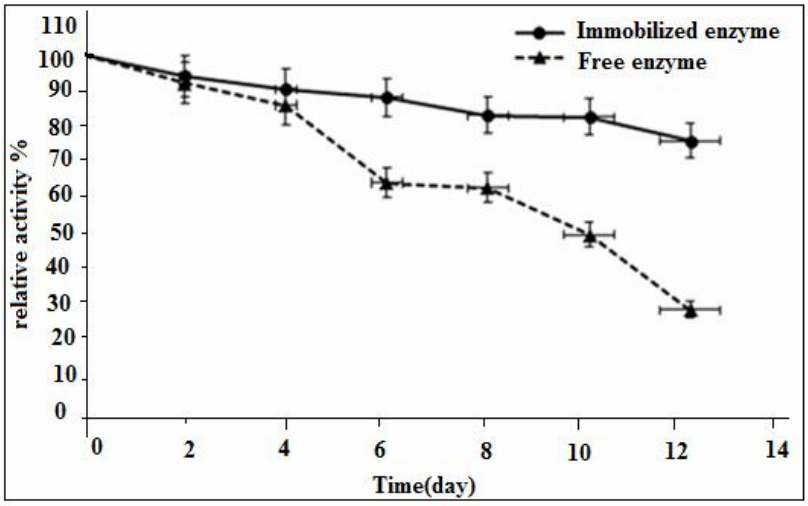

Fig. 9. Storage stability of the immobilized and free beta-amylase (the amount of beta -amylase: 150 µg, 10 mg of $ZnFe_2O_4$ nanoparticles in 20 mM phosphate buffer (pH = 7.0, t = 25 °C).

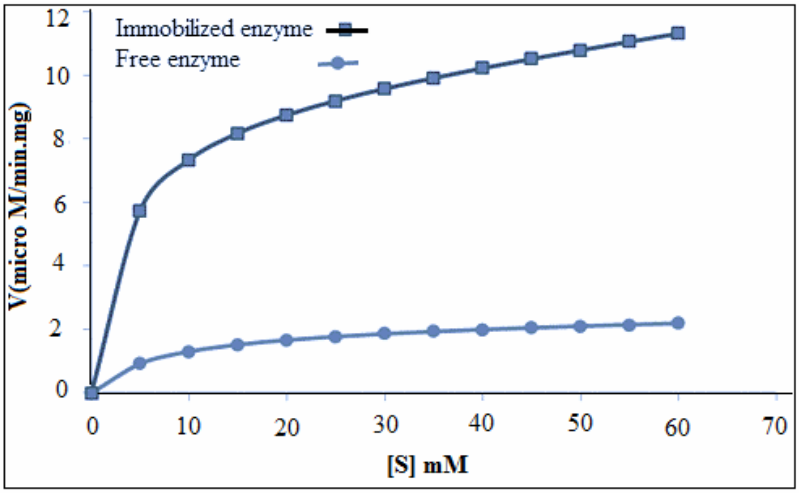

Fig. 10. Michaelis-Menten plot for free and immobilized beta-amylase (the initial amount of beta-amylase: 50 µg, 10 mg of $ZnFe_2O_4$ nanoparticles in 20 mM phosphate buffer (pH = 7.0, t = 25 °C).

CONCLUSIONS

In the present study, a novel magnetic support for immobilization of beta-amylase enzyme was synthesized with a simple and fast procedure. The covalent bonding increased the efficiency of enzyme immobilization and presence of $ZnFe_2O_4$ nanoparticles aided faster enzyme recovery. The activity of the immobilized enzyme was compared with the free enzyme and the reaction conditions were optimized. The immobilized enzyme was thermally more stable than the free enzyme. The maximum rate was found to increase for the immobilized enzyme [36-38]. The immobilized enzyme has also been efficiently recycled without the decreasing of activity after six cycles.

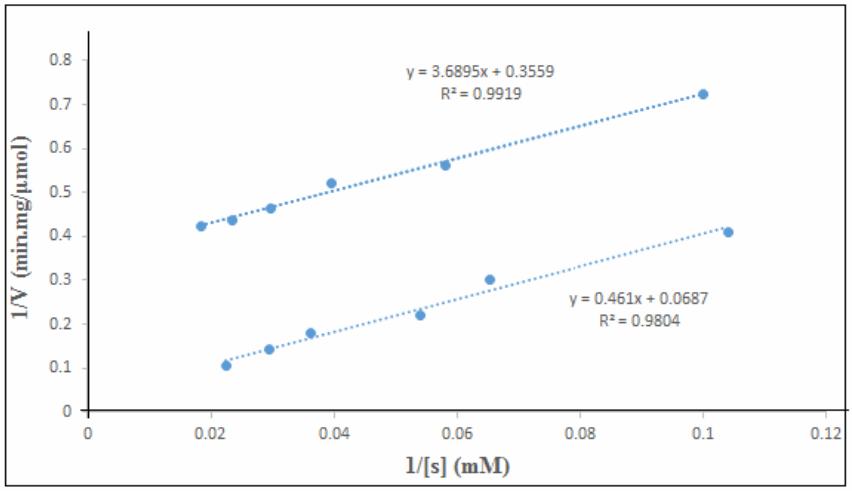

Fig. 11. Lineweaver-Burk plot for (a) free and (b) immobilized beta-amylase (the initial amount of beta-amylase: 50 µg, 10 mg of $ZnFe_2O_4$ nanoparticles in 20 mM phosphate buffer (pH = 7.0, t = 25 °C).

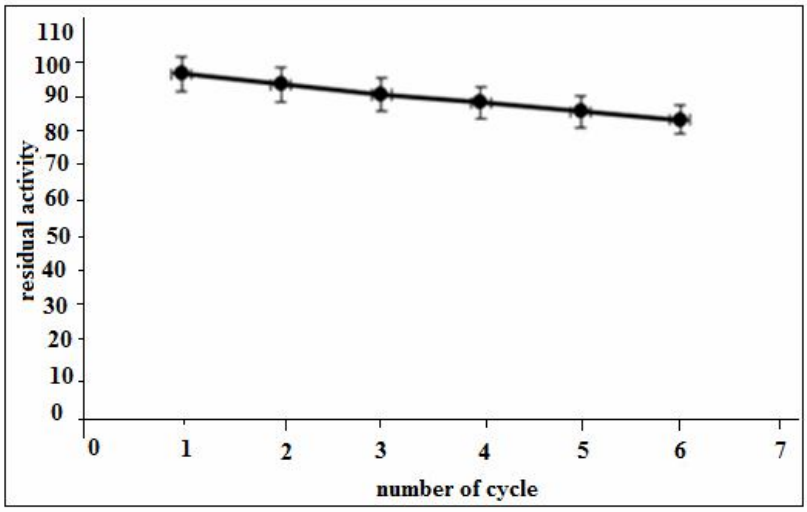

Fig. 12. Catalyst recycling of immobilized beta-enzyme. Immobilization conditions: t = 4 h, 10 mg of $ZnFe_2O_4$ nanoparticles in 20 mM phosphate buffer (pH = 7.0, t = 25 °C).

ACKNOWLEDGEMENTS

The financial support of the research council of Payame Noor University of Isfahan is gratefully acknowledged.

REFERENCES

[1] Zhao, C. X.; Yu, L.; Middelberg, A. P. J., Magnetic mesoporous silica nanoparticles end-capped with hydroxyapatite for pH-responsive drug release. *J. Mater. Chem. B*, **2013**, *1*, 4828-4833, DOI: 10.1039/C3TB20641F.

[2] Deng, Y.; Qi, D. W.; Deng, C. H.; Zhang, X. G.; Zhang, X. M.; Zhao, D. Y., Superparamagnetic high-magnetization microspheres with an Fe_3O_4@SiO_2 core and perpendicularly aligned

mesoporous SiO_2 shell for removal of microcystins. *J. Am. Chem. Soc.*, **2008**, *130*, 28-29, DOI: 10.1021/ ja0777584.

[3] Shen, J.; Zhu, Y.; Yang, X.; Zong, J.; Li, C., Multifunctional Fe_3O_4@Ag/SiO2/Au core-shell microspheres as a novel SERS-activity label *via* long-range plasmon coupling. *Langmuir*, **2013**, *29*, 690-695, DOI: 10.1021/la304048v.

[4] Liu, W.; Zhou, F.; Zhang, X. Y.; Li, Y.; Wang, X. Y.; Xu, X. M.; Zhang, Y. W., Preparation of magnetic Fe_3O_4@SiO_2 nanoparticles for immobilization of lipase. *J. Nanosci. Nanotechnol.*, **2014**, *14*, 3068-3072.

[5] Hou, C.; Zhu, H.; Wu, D. W.; Li, Y. J.; Hou, K.; Jiang, Y.; Li, Y. F., Immobilized lipase on macroporous polystyrene modified by PAMAM-dendrimer and their enzymatic hydrolysis. *Process Biochem.*, **2014**, *49*, 244-249.

[6] Marzia, M.; Vincent, C.; Sabino, V. V.; Manuel, A. V.; Julian, C.; Marc, R.; Carlos, J. S.; Morales, M. P., Large scale production of biocompatible magnetite nanocrystals with high saturation magnetization values through green aqueous synthesis. *J. Mater. Chem. B.*, **2013**, *1*, 5995-6004, DOI: 10.1039/ C3TB20949K.

[7] Gao, R. X.; Mu, X. R.; Zhang, J. J.; Tang, Y. H., Combination of surface imprinting and immobilized template techniques for preparation of core-shell molecularly imprinted polymers based on directly amino-modified Fe_3O_4 nanoparticles for specific recognition of bovine hemoglobin. *J. Mater. Chem. B*, **2014**, *2*, 1733-1741, DOI: 10.1039/C3TB21684E.

[8] Ujwal, S. P.; Qu, H. G.; Daniela, C.; Charles, J. C.; Arjun, S.; Cai, Y.; Tarr, M. A, Labeling primary amine groups in peptides and proteins with N-hydroxysuccinimidyl ester modified Fe_3O_4@SiO_2 nanoparticles containing cleavable disulfide-bond linkers. *Bioconjugate Chem.*, **2013**, *24*, 1562-1569, DOI: 10.1021/bc400165r.

[9] Govan, J.; Gun'ko, Y. K., Recent advances in the application of magnetic nanoparticles as a support for homogeneous catalysts. *Nanomater*, **2014**, *4*, 222-241, DIO: 10.3390/nano4020222.

[10] Yuan, Q.; Li, N.; Ceng, W. C.; Chi, Y.; Li, X. Y., Preparation of magnetically recoverable Fe_3O_4@SiO_2@Meso-TiO_2 nanocomposites with enhanced photocatalytic ability. *Mater. Res. Bull*, **2012**, *47*, 2396-2402, DOI: 10.1016/ j.materresbull.2012.05.031.

[11] Rodrigues, R. C.; Ortiz, C.; Berenguer-Murcia, A.; Torres, R.; Fernández-Lafuente, R., Modifying enzyme activity and selectivity by immobilization. *Chem. Soc. Rev.*, **2013**, *42*, 6290-6307, DOI: 10.1039/C2CS35231A.

[12] Garcia-Galan, C.; Berenguer-Murcia, A.; Fernandez-Lafuente, R.; Rodrigues, R. C., Potential of different enzyme immobilization strategies to improve enzyme performance. *Adv. Synth. Catal.*, **2011**, *353*, 2885-2904, DOI: 10.1002/adsc.201100534.

[13] Zhou, L. L.; Wu, J. J.; Zhang, H. J.; Kang,Y.; Guo, J.; Zhang, C.; Yuan, J. Y., Magnetic nanoparticles for the affinity adsorption of maltose bindingprotein (MBP) fusion enzymes. *J. Mater. Chem.*, **2012**, *22*, 6813-6818, DOI: 10.1039/C2JM16778F.

[14] Teng, Z. G.; Sun, C. H.; Su, X. D.; Liu, Y.; Tang, Y. X.; Zhao, Y. N.; Chen, G. T.; Yan, F.; Yang, N. N.; Wang, C. Y.; Lu, G., Superparamagnetic high-magnetization composite spheres with highly aminated ordered mesoporous silica shell for biomedical applications. *J. Mater. Chem. B.*, **2013**, *1*, 4684-4693, DOI: 10.1039/C3TB20844C.

[15] Min, D. D.; Zhang, X. D.; He, W.; Zhang, Y.; Li, P. W.; Zhang, M. M.; Liu, J. N.; Liu, S. J.; Xu, F. X.; Dua, Y.; Zhang, Z. J., Direct immobilization of glucose oxidase in magnetic mesoporous bioactive glasses. *Mater. Chem. B*, **2013**, *1*, 3295-3303, DOI: 10.1039/C3TB20480D.

[16] Li, Y.; Xu, X. Q.; Deng, C. H.; Yang, P. Y.; Zhang, X. M., Immobilization of trypsin on superparamagnetic nanoparticles for rapid and effective proteolysis. *J. Proteome Res.*, **2007**, *9*, 3849-3855, DOI: 10.1021/pr070132s.

[17] Karimi, M.; Keyhani, A.; Akram, A.; Rahman, M.; Jenkins, B.; Stroeve, P., Hybrid response surface methodology-genetic algorithm optimization of

ultrasound-assisted transesterification of waste oil catalysed by immobilized lipase on mesoporous silica/iron oxide magnetic core-shell nanoparticles. *Environ. Technol.*, **2013**, *34*, 2201-2211, DOI: 10.1080/09593330.2013.837939.

[18] Reddy, N. S.; Nimmangadda, A.; Sambasiva, R. K. R. S., An overview of the microbial α-amylase family. *Afr. J. Biotechnol.*, **2003**, *2*, 645-648.

[19] Schramm, M.; Loyter, A., Purification of a-amylases by precipitation of amylase-glycogen complexes. *Methods Enzymol.*, **1966**, *9*, 533-537, DOI: 10.1016/0076-6879(66)08095-9.

[20] Coutinho, P. M.; Reilly, P. J., Glucoamylase structural, functional and evolutionary relationships. *Protein Eng.* **1997**, *29*, 334-347, DOI: 10.1002/1097.

[21] de Souza, P. M.; de Oliveira Magalhães, P., Application of microbial α-amylase in industry-A review. *Braz. J. Microbiol.* **2010**, *41*, 850-61, DOI: 10.1590/S1517-83822010000400004.

[22] Atichokudomchai, A.; Jane, J.; Hazlewood, G., Reaction pattern of novel thermostable alpha-amylase. *Carbohydr. Polym.*, **2006**, *64*, 582-588, DOI: 10.1016/j.carbpol.2005.11.014.

[23] Morrison, T. A.; Pressey, R.; Kays, S. J., Changes in α- and β-amylase during Storage of Sweetpotato Lines with Varying Starch Hydrolysis Potential. *J. Am. Soc. Hortic Sci.*, **1993**, *118*, 236-242.

[24] Husain, S.; Jafri, F.; Saleemuddin, M., Effects of chemical modifications on the stability of invertase before and after immobilization. *Enzyme Microb. Tech.*, **1996**, *18*, 275-280, DOI: 10.1016/0141-0229(95)00119-0.

[25] Chen, X.; Lam, K. F.; Zhang, Q.; Pan, B.; Arruebo, M.; Yeung, K. L., Synthesis of highly selective magnetic mesoporous adsorbent. *J. Phys. Chem. C*, **2009**, *113*, 9804-9813, DOI: 10.1021/jp9018052.

[26] Jang, J.; Lim, H., Characterization and analytical application of surface modified magnetic nanoparticles. *Microchem. J.*, **2010**, *94*, 148-158, DOI: 10.1016/j.microc.2009.10.011.

[27] Abareshi, M.; Goharshadi, E. K.; Zebarjad, S. M.; Fadafan, H. K.; Youssefi, A., Fabrication, characterization and measurement of thermal conductivity of Fe_3O_4 nanofluids. *J. Magn. Magn. Mater.*, **2010**, *322*, 3895-3901, DOI: 10.1016/j.jmmm.2010.08.016.

[28] Rao, B. P.; Kumar, A. M.; Rao, K. H.; Murthya, Y. L. N.; Caltunb, O. F.; Dumitruc, I., Synthesis and magnetic studies of Ni-Zn ferrite nanoparticles. *J. Optoelectron Adv. M*, **2006**, *8*, 1703-1705.

[29] Stober, W.; Fink, A.; Bohn, E. J., Controlled growth of monodisperse silica spheres in the micron size range. *J. Colloid Interface Sci.*, **1968**, *26*, 62-69, DOI: 0.1016/0021-9797(68)90272-5.

[30] Wang, Y.; Liu, B., Conjugated polymer as a signal amplifier for novel silica nanoparticle-based fluoroimmunoassay. *Biosens. Bioelectron*, **2009**, *24*, 3293-3298, DOI: 10.1016/j.bios.2009.04.020.

[31] Sohrabi, N.; Rasouli, N.; Torkzadeh, M., Enhanced stability and catalytic activity of immobilized α-amylase on modified Fe_3O_4 nanoparticles. *Chem. Eng. J.*, **2014**, *240*, 426-433, DOI: 10.1016/j.cej.2013.11.059.

[32] Bradford, M. M., A rapid and sensitive method for the quantitation of microgram quantities of protein utilizing the principle of protein-dye binding. *Anal. Biochem.*, **1976**, *72*, 248-254.

[33] Bernfeld, P., Amylases α and β. *Methods Enzymol.*, **1955**, *1*, 149-158, DOI: 10.1016/0076-6879(55)01021-5.

[34] Li, X. Y.; Hou, Y.; Zhao, Q. D.; Teng, W.; Hu, X. J.; Chen, G. H., Capability of novel $ZnFe_2O_4$ nanotube arrays for visible-light induced degradation of 4-chlorophenol. *Chemosphere*, **2011**, *82*, 581-586, DOI: 10.1016/j.chemosphere.2010.09.068.

[35] Cao, X.; Gu, L.; Lan, X.; Zhao, C.; Yao, D.; Sheng, W., Spinel $ZnFe_2O_4$ nanoplates embedded with Ag clusters: Preparation, characterization, and photocatalytic application. *Mater. Chem. Phys.*, **2007**, *106*, 175-180, DOI: 10.1016/j.matchemphys.2007.05.033.

[36] Mukherjee, A. K.; Kumar, T. S.; Rai, S. K.; Roy, J. K., Statistical optimization of bacillus alcalophilus α-

amylase immobilization on iron-oxide magnetic nanoparticles, *Biotechnol. Bioprocess Eng.*, **2010**, *15*, 984-992, DOI: 10.1007/s12257-009-3160-7.

[37] Singh, V.; Singh, D., Polyvinyl alcohol-silica nanohybrids: An efficient carrier matrix for amylase immobilization, *Process Biochem.*, **2013**, *48*, 96-102, DOI: 10.1016/j.procbio.2012.10.017.

[38] Singh, V.; Kumar, P., Carboxymethyl tamarind gum-silica nanohybrids for effective immobilization of amylase, *J. Mol. Catal. B: Enzym.*, **2011**, *70*, 67-73, DOI: 10.1016/j.molcatb.2011.02.006.